# Diurnal Changes in Signal-to-Noise Ratio in a Distributed Acoustic Sensing System

Katherine E. Winters, Ph.D., P.E., M.ASCE[1]; Meghan C. Quinn, Ph.D., P.E.[2]; and Jennifer R. Piccuci, Ph.D.[3]

[1]Geotechnical and Structures Laboratory, US Army Engineer Research and Development Center, Vicksburg, MS. Email: katherine.e.winters@usace.army.mil
[2]Cold Regions Research and Engineering Laboratory, US Army Engineer Research and Development Center, Hannover, NH. Email: Meghan.C.Quinn@usace.army.mil
[3]Geotechnical and Structures Laboratory, US Army Engineer Research and Development Center, Vicksburg, MS. Email: Jennifer.R.Piccuci@usace.army.mil

## ABSTRACT

Distributed Acoustic Sensing (DAS) systems, typically consisting of a fiber-optic cable and an optical time-domain reflectometry interrogator, are commonly used to detect vibration in the medium surrounding the fiber-optic cable. DAS has been used for over a decade as a low-cost sensor for infrastructure monitoring in oil and gas pipelines. For confidence in DAS as an infrastructure monitoring system, it is important to recognize signal changes with time due to environmental effects. Previous research has explored the long-term changes in system performance. The purpose of this research is to document changes in DAS performance, with signal-to-noise ratio (SNR) in decibels (dBs) as the performance metric, for five data collections throughout each of two days approximately one month apart. One day was dry, and the other day was wet, having experienced over 3 in. (80 mm) of rainfall. The DAS system is installed in a trench containing gravel, sand, flowable fill, and native loess sections. Moisture and temperature sensors in each fill material report hourly average volumetric water content and soil temperature, while a nearby weather station collects hourly rainfall and air temperature data. A calibrated hammer on a metal plate was used to generate seismic waves directly above portions of the array in each fill material, thereby inducing vibrational strains in the fiber-optic cable. These signals were then compared to the noise in the associated cable section immediately before the hammer strike sequence. Results show significant changes in SNR values throughout the day. Consistent with previous research, the gravel trench had the strongest SNR, and the flowable fill had the weakest. While the test trenches were fully saturated on both study days, SNRs on the dry day (a day without precipitation) averaged several dBs higher than on the wet day (a day with precipitation). Variations in SNR within a material over the course of the day were significantly greater on the wet day than the dry day, but the variations within the day do not seem to be correlated to temperature or active rainfall. Understanding diurnal variations in DAS performance will inform the structural health monitoring community to better interpret system results.

## INTRODUCTION

Distributed Acoustic Sensing (DAS) is currently used for vibration monitoring applications such as pipeline monitoring, seismic activity monitoring, $CO_2$ sequestration monitoring, railway subgrade monitoring, and more (examples provided in Daley et al. 2016; Dou et al. 2017; Mateeva et al. 2014; Soga and Luo 2018). DAS typically consists of a fiber-optic cable and a fiber-optic analyzer (i.e., an interrogator; Soga et al. 2015). The fiber-optic cable serves as both the sensor and the vibration data transmission vehicle to the interrogator. For DAS, it is common to use an Optical Time-Domain Reflectometer (OTDR) interrogator that detects changes in Rayleigh scattering power that is proportional to the vibrational strain acting on the fiber optic cable (Krohn et al. 2014). The interrogator measures the power of the backscattered light and sorts the backscatter by return time. This return time is associated with a distance down the fiber optic cable. While state-of-the-art systems commonly now use phase-coherent DAS for wave-field analysis and subsurface characterization (Soga and Luo 2018; Wang et al. 2019), this study was undertaken with a legacy intensity-only OTDR interrogator in order to investigate direct surface signals.

DAS allows for continuous strain/vibration monitoring information to be acquired at a set spatial resolution (typically 2 to 10 m) over long distances at a high sampling rate (e.g., greater than 1,000 Hz). DAS response has been compared to accelerometers, geophones, and seismometers (Daley et al. 2016; Egorov et al. 2018).

Achieving consistent coupling between the fiber-optic cable and the soil remains a challenge for the DAS community. Poor coupling due to the development of air voids along the cable can cause improper transmission of seismic signals, thereby corrupting system performance. To evaluate DAS results and understand changes in response, it is important to study environmental effects, such as precipitation. Previous research explored the long-term changes in system performance (Quinn 2021). The purpose of this research is to document short-term (diurnal) changes in DAS performance, with signal-to-noise ratio (SNR) in decibels (dBs) as the performance metric for five data collections throughout each of two days approximately one month apart.

## METHODOLOGY

To study the effect of soil type and in situ aging on DAS response, as well as determine best practices for installation, a fiber-optic cable was installed in a trench with four fill materials:

1. Poorly graded gravel (GP) similar to Mississippi Department of Transportation roadway subgrade,
2. Poorly graded concrete sand (SP),
3. Flowable fill: a weak, excavatable concrete mixture,
4. Loess native to the site and representative of near-surface soil along the lower Mississippi River.

All were sourced from a supplier local to Vicksburg, MS. At the time of the system installation, it was theorized that the flowable fill would perform well due to its rigidity, while the native material was taken as a baseline and not expected to provide high SNR values due to historical site performance. While it is important to consider the effect of the impedance ratio(s) between where the source is occurring and where the fiber optic cable is placed for complex geophysical investigations, the scope of this study focuses on resulting SNR-related performance from plausible, readily available installation options without explicit concern for impedance mismatch between soil types.

The cable used for this study was an industry standard, armored, 24-strand fiber-optic cable with a rubber-coated exterior. The exterior diameter was 0.50 in. A conventional, incoherent, not-phase-sensitive OTDR interrogator was used to generate and receive signals throughout the array. Cable was installed at a depth of 2 ft through 100-ft sections in each of the gravel, sand, flowable fill, and native loess materials in trenches 3 ft deep by 1 ft wide (Winters et al. 2020).

A calibrated drop hammer was the impact source for this study. The hammer was used to strike a metal plate at two consistent locations above each fill material trench. At each hammer location, ten hammer strikes were performed. The hammer strike locations were approximately above the buried fiber-optic cable.

Data were collected on two days, one month apart. One day was dry (no precipitation) with dry surface conditions, while the other day experienced over 3 in. (80 mm) of rainfall and very wet surface conditions. Air temperature on the surface dry day began at 1.6 degrees Celsius at 0900 and rose to 18.9 degrees Celsius at 1600. On the surface wet day, the temperature ranged from 17.8 to 23.0 degrees Celsius during the data collection hours. On both days, the soil temperature at the level of the cable was constantly approximately 14 degrees Celsius. The volumetric water content on both days was 0.44 for gravel, 0.29 for sand, 0.33 for flowable fill, and 0.43 for the native loess material. Water content variations at the level of the sensor within days and between the two study periods were both within the instrument's measurement error range (<+/- 0.01). Longer-term monitoring at this site suggests that the fiber-optic cable is continually below the water table during winter months, including this study period.

Data were plotted using MATLAB (as shown in Figure 1) for 12 channels in the test bed; each channel is 10 m long. The channels located in the testbed, starting from the bottom of the plot, are shown as dark blue for gravel, green for sand, dark red for flowable fill, and purple for the native loess material. The strongest sets of hammer strikes based on multiple data collections were processed for each fill material (i.e., the most distinct spikes based on visual inspection for the gravel trench were the first set of hammer strikes on the bottom channel of Figure 1). The hammer hits selected for analysis are circled. The channels are offset with arbitrary y-axis values in the display for clarity.

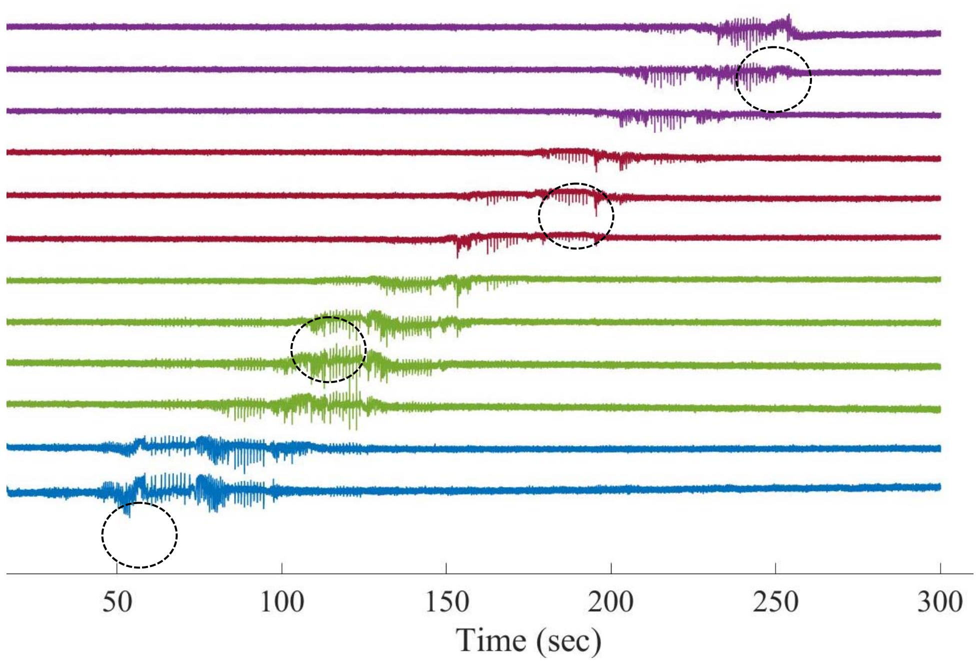


**Figure 1. MATLAB plot showing hammer hits on 11 channels in the testbed. Dark blue for gravel, green for sand, dark red for flowable fill, and purple for the native loess material.**

Figure 2 shows a typical response in a sand channel to one ten-strike sequence. Ten major peaks can be seen corresponding to the hammer strikes. There are also minor peaks before the major peaks. These are hypothesized to be the hammer striking the top of the sleeve but were cropped out for the analysis.

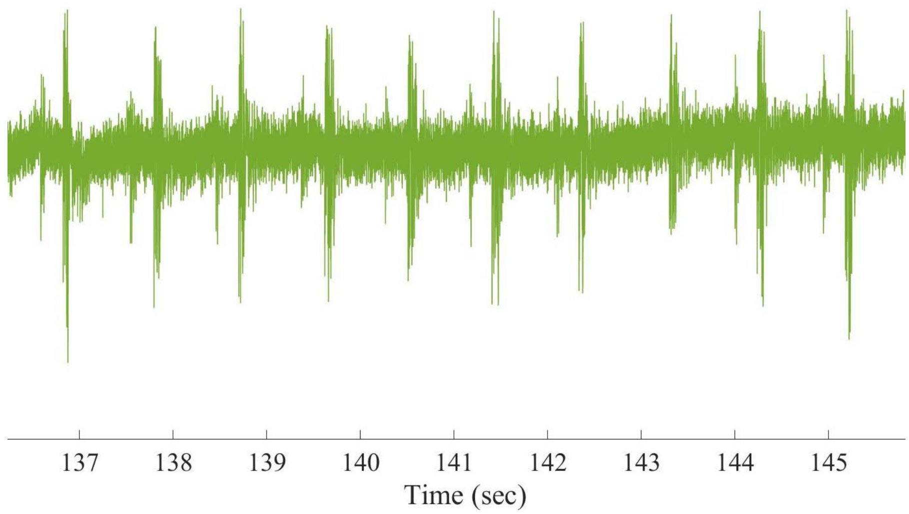


**Figure 2. MatLab view of one set of 10 hammer hits in the sand trench.**

Signal-to-Noise Ratio (SNR), as defined in Equation 1, was used to evaluate the performance of DAS channel by channel. SNR is defined as a logarithmic measure of the ratio of the Root Mean Square (RMS) values of the signal and the noise. A 0.30-sec capture of the signal is used to calculate $RMS_{signal}$ , whereas a 0.30-sec capture of the noise immediately before the series of hits is used to calculate $RMS_{noise}$. Each capture period was identified by a researcher based on plots similar to Figure 2. The capture length (i.e., the time window) was selected as a consistently achievable signal capture time and noise capture time that could be used across all data sets at each location.

$$SNR\ (dB) = 20\ log_{10}\left(\frac{RMS_{signal}}{RMS_{noise}}\right) \quad (1)$$

**Table 1. Signal-to-Noise Ratio and Standard Deviation under dry surface conditions.**

| | Average SNR (dB) | | | | Standard Deviation (dB) | | | |
|---|---|---|---|---|---|---|---|---|
| Time | Gravel | Sand | Flowable Fill | Native Loess | Gravel | Sand | Flowable Fill | Native Loess |
| 9:00 | 11.86 | 8.37 | 4.59 | 7.48 | 0.92 | 0.60 | 0.73 | 0.52 |
| 11:00 | 9.29 | 8.47 | 3.08 | 6.91 | 1.03 | 0.75 | 0.35 | 1.25 |
| 13:00 | 8.71 | 6.41 | 5.47 | 10.93 | 0.67 | 1.20 | 1.14 | 0.74 |
| 14:00 | 9.85 | 8.55 | 5.46 | 8.48 | 0.48 | 0.36 | 0.28 | 0.45 |
| 16:00 | 7.80 | 6.79 | 3.69 | 7.16 | 0.32 | 0.61 | 0.27 | 1.33 |
| Average | 9.50 | 7.72 | 4.46 | 8.19 | 0.68 | 0.71 | 0.55 | 0.86 |

## RESULTS

Results show significant changes in SNR values throughout the day. Tables 1 and 2 present the average SNR and standard deviation for each data collection period for dry surface and wet surface conditions, respectively.

**Table 2. Signal-to-Noise Ratio and Standard Deviation under wet surface conditions.**

| | Average SNR (dB) | | | | Standard Deviation (dB) | | | |
|---|---|---|---|---|---|---|---|---|
| Time | Gravel | Sand | Flowable Fill | Native Loess | Gravel | Sand | Flowable Fill | Native Loess |
| 9:00 | 6.40 | 1.88 | 0.83 | 4.51 | 0.92 | 0.60 | 0.73 | 0.52 |
| 11:00 | 3.78 | 1.73 | 2.14 | 2.23 | 0.97 | 0.62 | 0.24 | 0.29 |
| 13:00 | 2.80 | 2.61 | N/A | 1.16 | 0.38 | 0.39 | N/A | 0.43 |
| 14:00 | 4.92 | 4.09 | 0.63 | 3.21 | 0.35 | 0.43 | 0.41 | 0.38 |
| 16:00 | 3.66 | 3.05 | N/A | 1.70 | 0.30 | 0.18 | N/A | 0.29 |
| Average | 4.31 | 2.67 | 1.20 | 2.56 | 0.58 | 0.44 | 0.46 | 0.38 |

The SNRs for each hit are plotted in Figures 3-6. The dry surface day is plotted with box markers while the wet surface day is plotted with triangles. The dry surface values are consistently higher than the wet surface values.

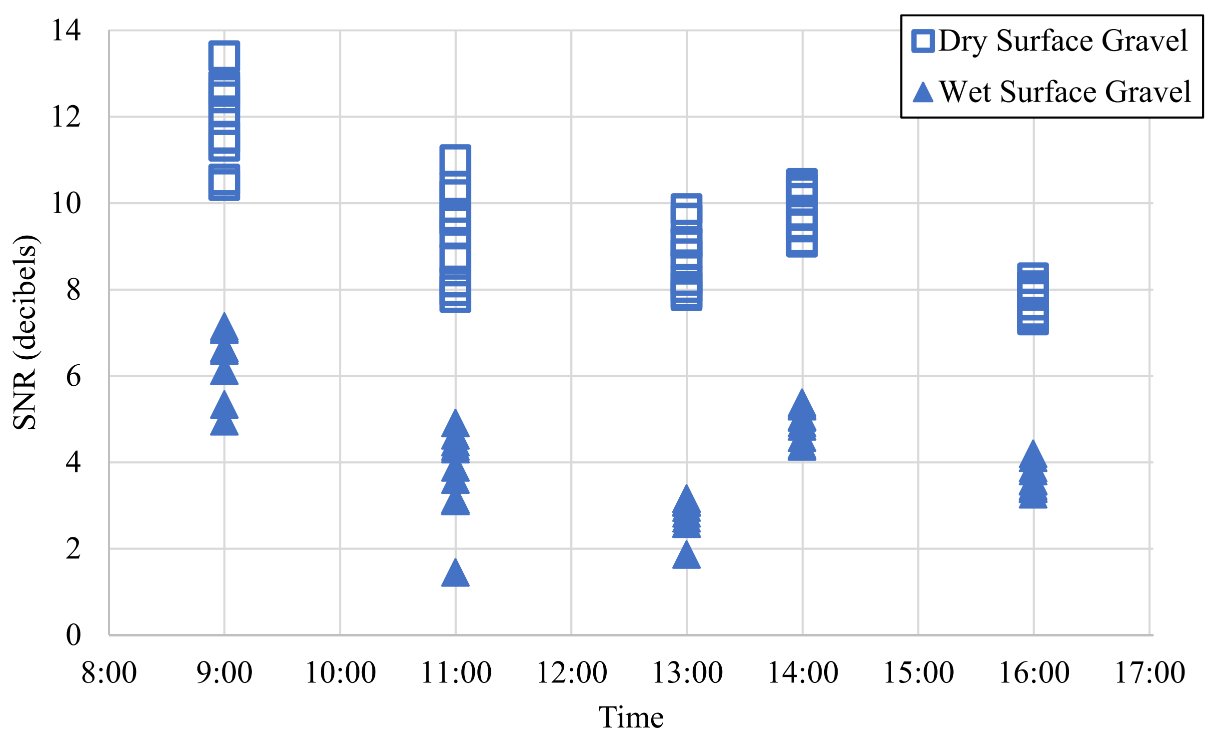


**Figure 3. Signal-to-Noise (SNR) Ratio in Gravel Trench.**

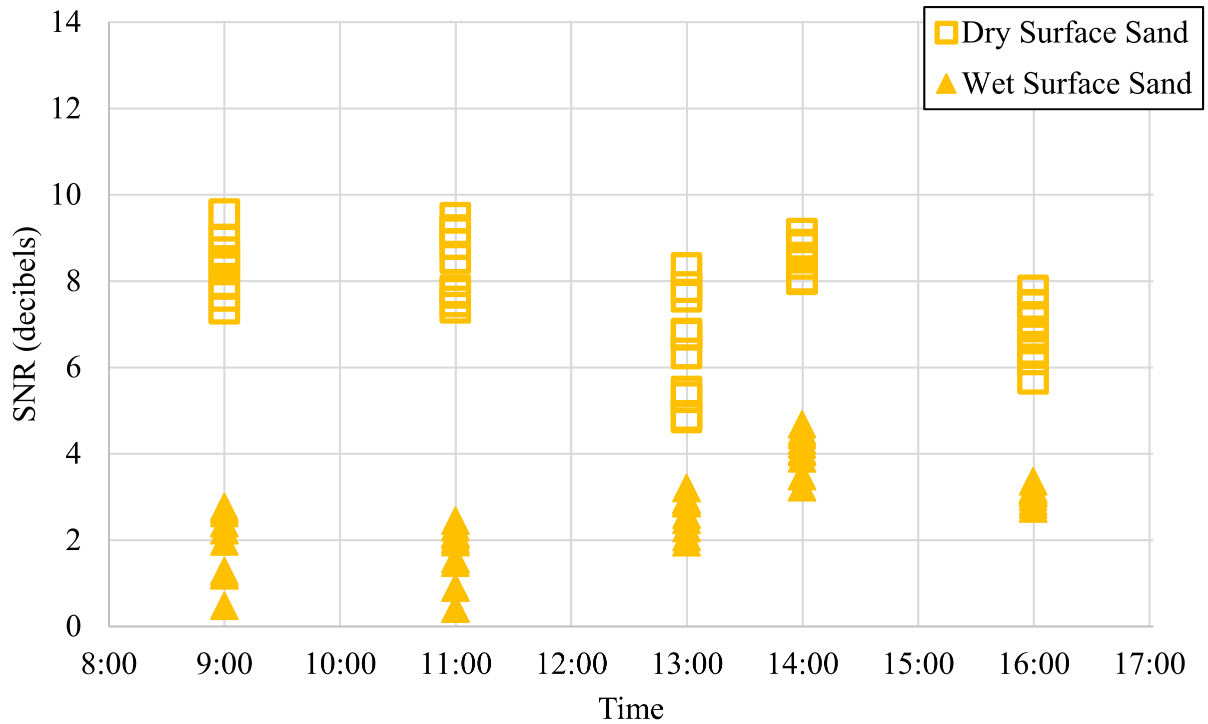


**Figure 4. Signal-to-Noise (SNR) Ratio in Sand Trench.**

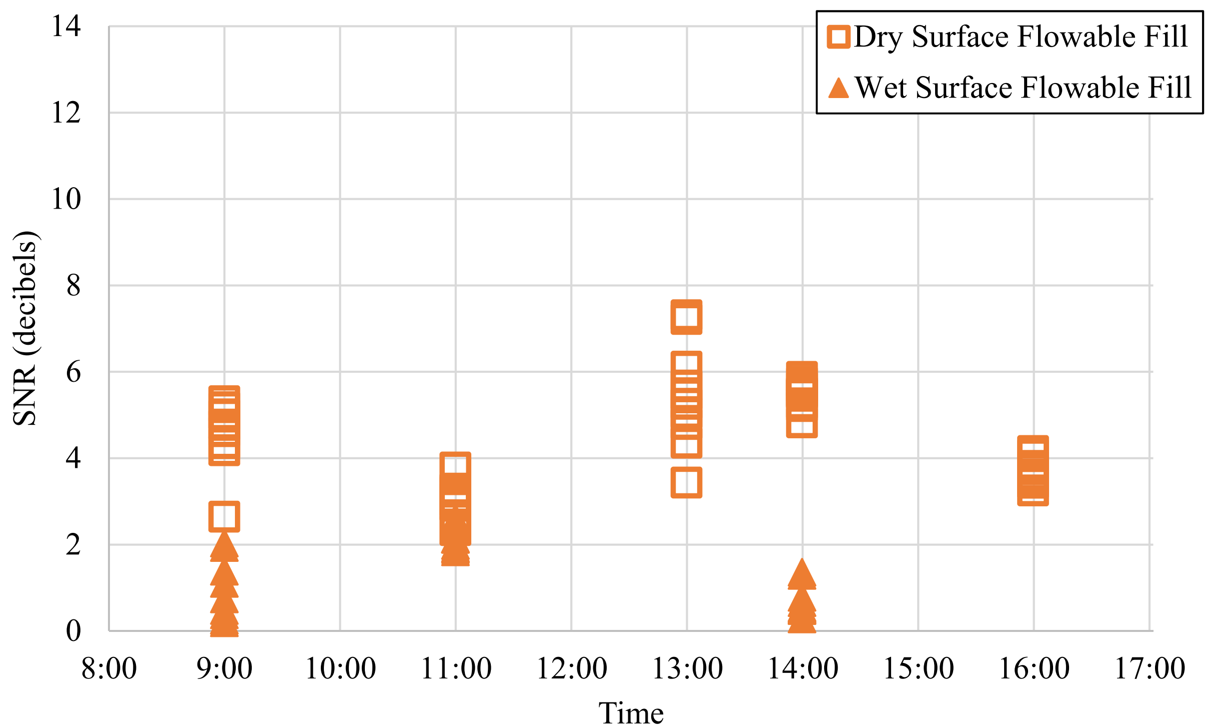


**Figure 5. Signal-to-Noise (SNR) Ratio in Flowable Fill Trench.**

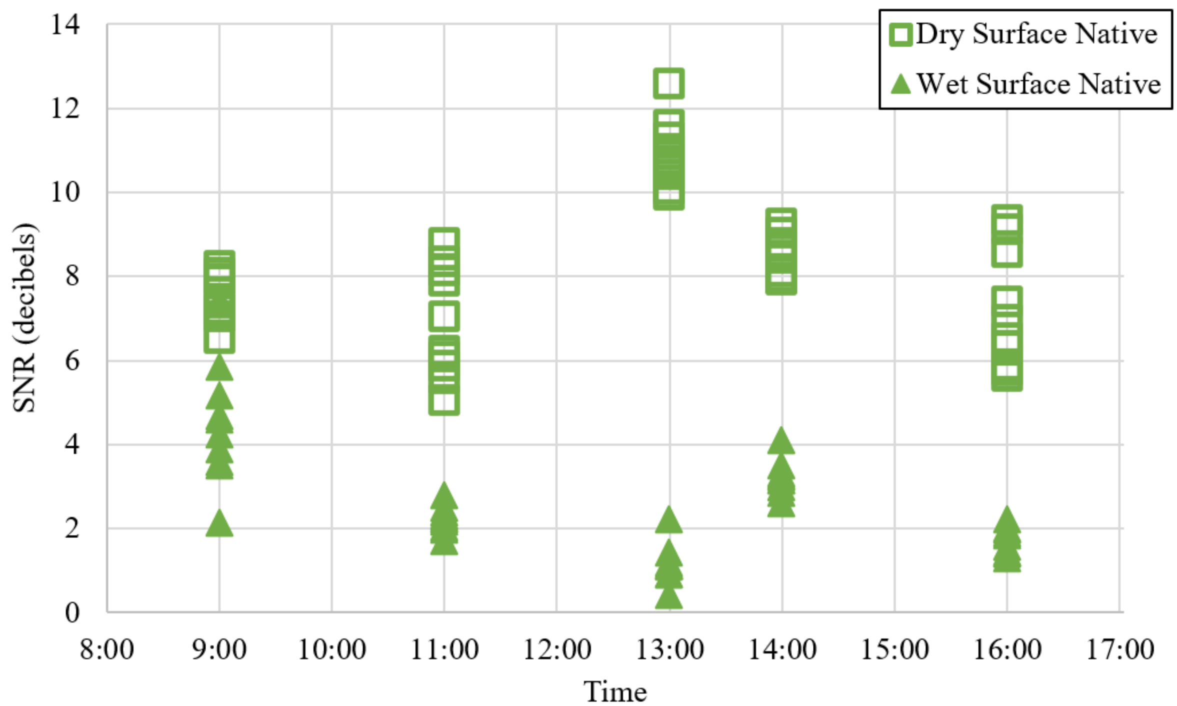


**Figure 6. Signal-to-Noise (SNR) Ratio in Native Loess Trench.**

## CONCLUSIONS

Consistent with previous research (Quinn 2021), the gravel trench had the highest SNR and the flowable fill had the lowest. While the test trenches were fully saturated at the level of the cable on both study days, SNRs on the dry surface day averaged several dB higher than on the wet surface day. Variations in SNR within a material over the course of the day were significantly greater on the wet surface day than the dry surface day, but the variations within the day do not seem to be correlated to temperature or active rainfall.

For the purposes of infrastructure monitoring, it is important to note that SNR values for the same source can vary by several dBs within a few seconds of a series of 10 hammer hits. Surface moisture conditions also greatly impact the magnitude of the signal despite the soil temperature and moisture content being constant at the level of the sensor. Future research is suggested for variations in soil conditions at the sensor. An intensity-only OTDR DAS interrogator was used for this effort which means that only signal amplitude is measured and comparable. Some of the work cited herein (e.g. Daley et al. 2016; Dou et al. 2017; Egorov et al. 2018; Mateeva et al. 2014.) used a coherent OTDR DAS interrogator which is phase sensitive and often used for geophysics applications such as evaluation of seismic waves for subsurface site investigation. A coherent OTDR DAS interrogator would allow for greater geophysical subsurface characterization but is not expected to change any of the key findings since the amplitude of the signal was used to calculate SNR.

## ACKNOWLEDGEMENTS

The authors wish to thank A. Dulaney for his contributions. Permission to publish was granted by Director, Geotechnical and Structures Laboratory, with unlimited distribution.

## REFERENCES

Daley, T. M., Miller, D. E., Dodds, K., Cook, P., and Freifeld, B. M. (2016). "Field testing of modular borehole monitoring with simultaneous distributed acoustic sensing and geophone vertical seismic profiles at Citronelle, Alabama." *Geophysical Prospecting*, (64) 1318-1334.

Dou, S., Lindsey, N., Wagner, A. M., Daley, T., Thomas, M., Freifeld, B., Robertson, M., Peterson, J., Ulrich, C., Martin, E. R., and Ajo-Franklin, J. B. (2017). "Distributed acoustic sensing for seismic monitoring of the near surface: A traffic-noise interferometry case study." *Scientific Reports*, (7)

Egorov, A., Correa, J., Bóna, A., Pevzne, R., Tertyshnikov, K., Glubokovskikh, S., Puzyrev, V., and Gurevich, B. (2018). "Elastic full-waveform inversion of vertical seismic profile data acquired with distributed acoustic sensors." *Geophysics*, (83)3,

Krohn, D., MacDougall, T., and Mendez, A. (2014). *Fiber Optic Sensors: Fundamentals and Applications, Fourth Edition*. Bellingham, Washington: SPIE Press.

Mateeva, A., Lopez, J., Potters, H., Mestayer, J., Cox, B., Kiyashchenko, D., Willis, P., Grand, S., Hornman, K., Kuvshinov, B., Berlang, W., Yang, Z., and Detomo, R. (2014). "Distributed acoustic sensing for reservoir monitoring with vertical seismic profiling." *Geophysical Prospecting*, 62, 679–692,

Quinn, M. C. L. (2021). "Geotechnical Effects on Fiber-Optic Distributed Acoustic Sensing Performance." Open Access Dissertations. Paper 1238. https://digitalcommons.uri.edu/oa_diss/1238.

Soga, K., Kwan, V., Pelecanos, L., Rui, Y., Schwamb, T., Seo, H., and Wilcock, M. (2015). "The role of distributed sensing in understanding the engineering performance of geotechnical structures." *Proceedings Geotechnical Engineering for Infrastructure and Development*. ISBN 978-0-7277-6067-8.

Soga, K., and Luo, L. (2018). "Distributed fiber optics sensors for civil engineering infrastructure sensing." *Journal of Structural Integrity and Maintenance*, (3), 1, 1-21.

Wang, Y., Yuan, H., Liu, X., Bai, Q., Zhang, H., Gao, Y., and Jin, B. (2019). "A comprehensive Study of Optical Fiber Acoustic Sensing." *IEEE Access*, (7) 85821-85837.

Winters, K. E., Quinn, M. C., and Taylor, O. D. S. (2020). "Assessing the frictional resistance between fiber-optic sensor cable and different soil types." In *Geo-Congress 2020: Modeling, Geomaterials, and Site Characterization* (164-171). Reston, VA: American Society of Civil Engineers.